MDPI

Article

Research on the Friction and Wear Properties of Dents Textured Rolling Element Bearings under Dry Wear

Shaoni Sun [1], Risheng Long [2],*, Zhihao Jin [2], Yimin Zhang [2], Zichen Ju [2] and Xuanying Du [3]

[1] School of Mechanical Engineering and Automation, Northeastern University, Shenyang 110819, China; shnisun@me.neu.edu.cn
[2] Equipment Reliability Institute, Shenyang University of Chemical Technology, Shenyang 110142, China; jzh_sict_ln@sina.com (Z.J.); zhangyimin@syuct.edu.cn (Y.Z.); mozaiyinianting@163.com (Z.J.)
[3] School of Foreign Languages, Shenyang University of Chemical Technology, Shenyang 110142, China; duxuanying@syuct.edu.cn
* Correspondence: etomi@163.com

Abstract: To explore the effect of dents on the tribological behavior of the "washers-cage-rollers" system of rolling element bearings (REBs), the friction and wear properties of dents textured thrust cylindrical roller bearings (81107TN) with different diameters of dents (DAOD, 200, 250, 300 μm), depth of dents (DPOD, 4, 8, 12 μm) as well as circumferential interval angle (CFIA, 1.5°, 2.0°, 2.5°) were researched under dry wear. The surface stresses of REBs and the influence mechanism of dents were also compared and discussed. The results show that: due to the nylon film formed and left on the raceways, the coefficients of friction (COFs) of dents textured bearings are all higher than the average COF of smooth ones, while their wear losses may become higher or lower, depending on the combination of pattern parameters. The influence of the DPOD on the tribological performance of textured bearings is more significant than that of the DAOD. The results show that, when the DAOD and DPOD are 250 and 8 μm, respectively, compared with the smooth ones, the mass losses of bearings can be reduced by up to 49.22% under dry wear, which would be an important reference for the optimal design of the "washers-cage-rollers" system of REBs.

Keywords: rollingelement bearing; tribological behavior; surface texturing; dents; dry wear

1. Introduction

Rolling element bearings (REBs) are mainly applied to the rotating machinery, e.g., internal combustion engines, turbines, aero-motors, electric motors, gearboxes, machine tools (lathes, millers, borers, drillers, etc.), to support shafts or restrict their movements in the axial direction. REB is budget, but its failure may be costly. Fatigue wear and abrasive wear, usually caused by the contamination and deterioration of lubricating oil, bad lubrication, poor fits, and misalignment s, are the final failure mode of REBs [1,2]. Based on the published data, more than 40% of the downtime of induction motors should be attributed to bearing failure [3]. Therefore, it is meaningful to enhance the friction and wear properties of REBs, and further improve their effective service lives.

Actually, the friction and wear properties of sliding/rolling surfaces are commonly determined by their surface characteristics, (e.g., roughness, hardness), contact type, (i.e., point, line, and surface), lubrication regime, and the materials [4–6]. So, surface texture (ST) is introduced and widely applied to fabricate different units, (e.g., dents, grooves, grids), and has proved to be a cost-effective and fast means to control the tribological behavior of mechanical components, e.g., sliding-bearing [7], journal-bearing [8,9], cylinder liner-piston ring of internal combustion engines [10], under different lubrication regimes [11–17]. Dents are the commonly used unit-types and they are usually distributed in a pattern on the surface of materials, (e.g., metals [18,19], ceramics [20], polymers [21]).

Over the past 60 years, most publications about REBs are focused on their rolling contact fatigue (RCF), theoretical calculation, and fault diagnosis. Only a few works investigated the tribological behavior of REBs [22]. On the wear behavior, El-Thalji I., etc., proposed a five-stage model to reveal the wear-interactions and evolution of bearings over the whole lifetime, i.e., running-in stage, steady-state stage, defect-initiation stage, defect-propagation stage, and damage-growth stage [23]. The wear mechanisms of the five stages, the interaction among mechanisms, the surface-topology changes, and the key factors in each stage were also illustrated. Winkler et al. reported a numerical procedure to study the wear evolution of thrust cylindrical roller bearing (TCRB, 81212) in the mixed elastohydrodynamically lubrication (EHL) through a three-dimensional EHL model based on the finite element (FE) method, considering realistic geometry and locally varying velocities [24]. Rosenkranz et al. processed some dot-like patterns (periodicity of 6.5 μm and depth of 1 μm) on the raceways of 81,212 bearings. Compared with the average wear loss of smooth ones, an 83% reduction in the mass loss of dots textured bearings was finally obtained [25]. Vidyasagar et al. fabricated bionic patterns inspired by the skin of Dendroaspispolylepis and micro-dimples on the raceways of inner races of deep groove bearings and tested them at different rotational speeds (1.2–3.4 m/s) and loads (20–60 N) [26,27]. Long et al. researched the tribological behavior of grooves/leaf-vein textured TCRBs (81107TN) under dry wear or starved lubrication, with a fixed or periodical varying axial load [28–32]. Considering the high amount of sliding (due to the kinematical slip) at both ends of rollers, the functioning of surface textures in cam-tappet contacts with high slip-rolling researched by Marian et al. is also of great reference value [33]. However, the friction and wear properties of dents textured rolling element bearings and the influence mechanism of dents on their tribological behavior are both not clear yet, especially under dry wear.

Therefore, based on previous works [34,35], different dent patterns were textured on the shaft washers of TCRBs, which are commonly used in machines/tools, (e.g., internal-combustion engines, hydraulic impact equipment) to withstand huge axial loads, by laser-marking equipment (PL100–30W, Shenyang Sepbase, China). Dry wear is the worst work condition for all bearings. For example, when a jet fighter is doing tumbling, tail slide, or Pugachev Cobra maneuver, the aviation rolling element bearings of the engine have to work under starved lubrication or even dry wear for a while (<30 s). So, the tribological performances of dents textured bearings under dry wear were researched in this work to reveal the wear-resistance and friction reduction ability of the texture units. The static surface stresses and the influence mechanism of dents on the friction and wear properties of rolling element bearings were also studied and discussed, which would be an important reference for the optimal design of their raceways.

2. Materials and Modeling

In this work, 81107TN bearings (YFB, Changzhou, China) were used [28–32]. Their dimensions include: external diameter of washers (both the shaft and seat), 52 mm; internal diameter of shaft washer, 35 mm; internal diameter of seat washer, 37 mm; diameter of rollers, 5 mm; height of rollers, 5 mm; height of washers (both the shaft and seat), 5 mm. The material of those metal parts (shaft washer, seat washer, and cylindrical rollers) is GCr15 (SAE52100) with a surface hardness of HRC 62 ± 1. The cage is made of nylon (PA66, black). Compared with the sheer rolling friction, the wear behavior of TCRBs, rolling combined with sliding, is more complex, especially under dry wear.

Dents are only textured on the raceways of shaft-washers by fiber laser, with a power of 30 W, a scanning-speed of 15 mm/s, and a frequency of 1000 kHz. The wavelength of laser is 1064 μm. As displayed in Figure 1, there are three key parameters of one pattern: the diameter of dents (DAOD, 200, 250, 300 μm), the depth of dents (DPOD, 4, 8, 12 μm) as well as the circumferential interval angle (CFIA, 1.5°, 2.0°, 2.5°). Through repeated tests, the distance between two adjacent dents is set as a constant, 0.89 mm. Among three parameters, DAOD and CFIA are the key ones to control the area-density of textured

raceways. Based on the values of DAOD, CFIA, and DPOD, dents textured TCRB groups are marked from T01 to T11 (see Table 1), and each group includes three bearings. A smooth group is introduced to be a reference and coded as T12. Therefore, a total of 72 ($12 \times 3 \times 2$) 81107TN bearings were consumed in this work.
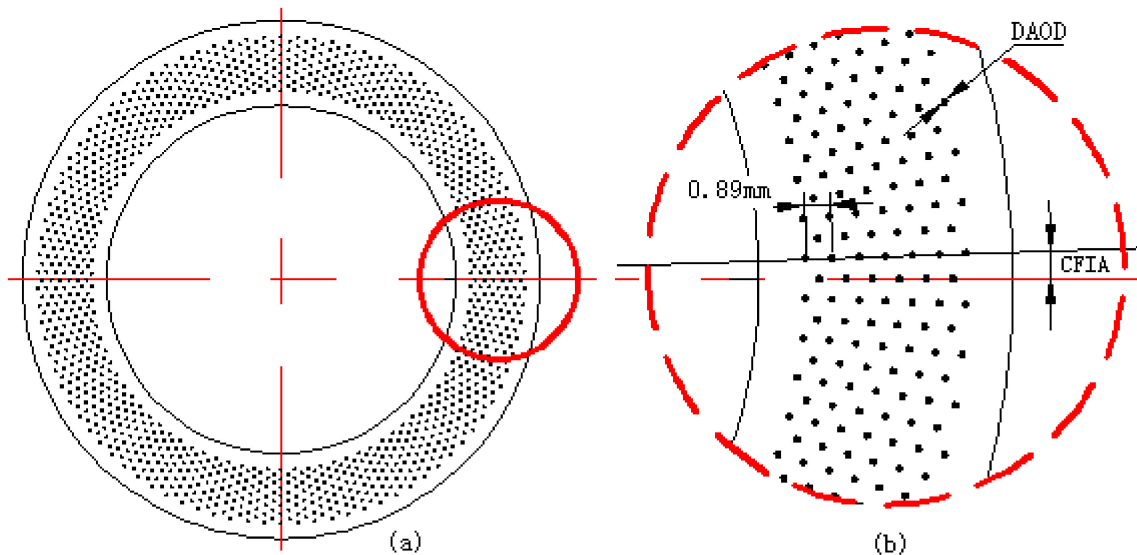

Figure 1. Texture pattern of the shaft washer of 81107TN bearing and the key parameters. (**a**) Top view of dents textured raceway; (**b**) local magnification of the red circle.

Table 1. Parameters of 81107TN bearing groups.

Group No.	DAOD (μm)	DPOD (μm)	CFIA (°)	Area Density (%)	τ
T01	200	4	2.0	3.17	0.50
T02	200	8	2.0	3.17	1.00
T03	200	12	2.0	3.17	1.50
T04	250	4	2.0	4.95	0.78
T05	250	8	2.0	4.95	1.56
T06	250	12	2.0	4.95	2.34
T07	300	4	2.0	7.12	1.13
T08	300	8	2.0	7.12	2.25
T09	300	12	2.0	7.12	3.38
T10	300	8	1.5	9.49	3.00
T11	300	8	2.5	5.70	1.80
T12	—	—	—	—	—

Furthermore, to reflect the debris-collection capacity of dents textured bearings, the effective volume coefficient of dents (EVCD) is also introduced and defined as follows [31]:

$$\tau = \frac{2 \times DAOD^2 \times DPOD}{CFIA \times 0.2^2 \times 8} = \frac{DAOD^2 \times DPOD}{CFIA \times 0.2^2 \times 4} \tag{1}$$

All bearings are handled according to the following steps prior to wear tests: first, remove the antirust oil of bearings; second, process dents on the raceways of the shaft washers of T01-T11 bearings; third, polish the textured surfaces with metallographic sandpapers; finally, wash them in an ultrasonic tank and dry them by a hot blower. A wear tester (MMW-1A, Huaxing, Jinan, China) was chosen to obtain the friction and wear properties of dents textured TCRBs under dry wear with a vertical loading force of 2950 ± 100 N and a rotating speed of 250 RPM (revolutions per minute), using a customized tribo-pair for 81,107 bearings [28–30]. The duration of each test is 18,000 s, which is restricted

by the number of samplingpoints as well as the longest continuous test time of bearings in this condition. Each group (T01-T12) was tested three times using three bearings. When one test is finished, a high-precision electronic analyticalbalance (EX225D, Ohaus, Parsippany, NJ, USA, 0.1 mg/120 g) is used to measure the mass loss of sample, (i.e., the original mass of shaft washer minus its mass after test), and a 3D non-contact surface microscope (VK-1050, Keyence, Osaka, Japan, laser/white-light) is used to observe the worn surface.

In addition, a three-dimensional FE model of 81107TN bearings was created through ANSYS Workbench [31]. Static-structural simulations were conducted under the same axial load, i.e., 2950 N. The bottom of the seat washer was constrained in three directions. To further analyze the difference insurface stresses among the textured groups, a radial path was set on the raceway of the shaft washer. The angle between the path and the horizontal line is 0.4° to ensure that the path exists for all bearings (T01–T11) but does not pass through any dent [31].

3. Experimental and Simulation Results

3.1. COFs

Figure 2 shows the COF curves of T01-T12 under dry wear. Note that: The COF curve of each group is the mean curve of three tests. To better compare the COF difference of bearings, the curve and the average-COF line of the smooth group are both added as references. The label "TXX: XXX-X" in the figure means "Group code: DAOD-DPOD". As shown in the figure, the COFs of T01-T11 are all higher than that of T12 (smooth). Specifically, compared with the coefficients of T01 and T02, when the DAOD is 200 μm, the COF of T03 is the lowest (see Figure 2a). When the DAOD is 250 μm, the COF of T05 is lower than those of T04 and T06 (see Figure 2c). As the DAOD is 300 μm, the curves of T07, T08, and T09 are disordered and almost mix together first (see Figure 3e, 0–11,000s), but the COF of T08 becomes much smaller than those of T07 and T09 in their latter periods (11,000–18,000 s). Likewise, when the DPOD is 4 μm, the curves of T01, T04, and T07 are almost the same (see Figure 2b). When the DPOD is 8 μm, the COF of T05 is lower than those of T02 and T08 (see Figure 2d). When the DPOD is 12 μm, the COF of T03 is the lowest among T03, T06, and T09 (see Figure 2f).

The COF curves of bearings (T10, T08, and T11) with different CFIAs (1.5°, 2°, 2.5°) under dry wear are shown in Figure 2g. Three groups have the same DAOD (300 μm) and DPOD (8 μm). As shown in the figure, among T10, T08, and T11, the average-COF of T11 is the lowest, while that of T08 is the highest. However, the difference betweenthe three curves is quite small.

3.2. Worn Surfaces and Mass Losses

The ultrasonic washed worn surfaces of T01-T12 under dry wear are shown in Figure 3. Owing to the huge friction-induced heat, there are high-temperature marks on the worn surfaces of all groups. Figure 4 shows the average mass losses (shaft washers) and average-COFs of T01-T12. Note that the wear loss of each group is also the average of three tests. As shown in the figure, the wear loss of T08 is the lowest in all groups, whether the textured or smooth. This is the reason forthe parameter selection of T10 and T11. The mass losses of T02, T05, and T09 are also much lower than those of other bearings.

3.3. Equivalent Stresses of Dents Textured "Washers-Cage-Rollers" System

Figure 5 shows the equivalent stress curves along the paths of T01-T12. Apparently, due to the "edge crushing" of both ends of cylindrical rollers, there are two equivalent stress peaks onboth sides of the raceways and the right peak (outer side) ismuch higher than the left one (inner side). The stresses in the contact region between cylindrical rollers and the raceway are much greater than those in other areas. Compared with the smooth group, the equivalent stresses of textured bearings are 4~5 times larger and their peakstresses can be even up to 53.37 MPa. This is because the effective contact area between the raceway and rollers of dents textured bearing is significantly reduced.
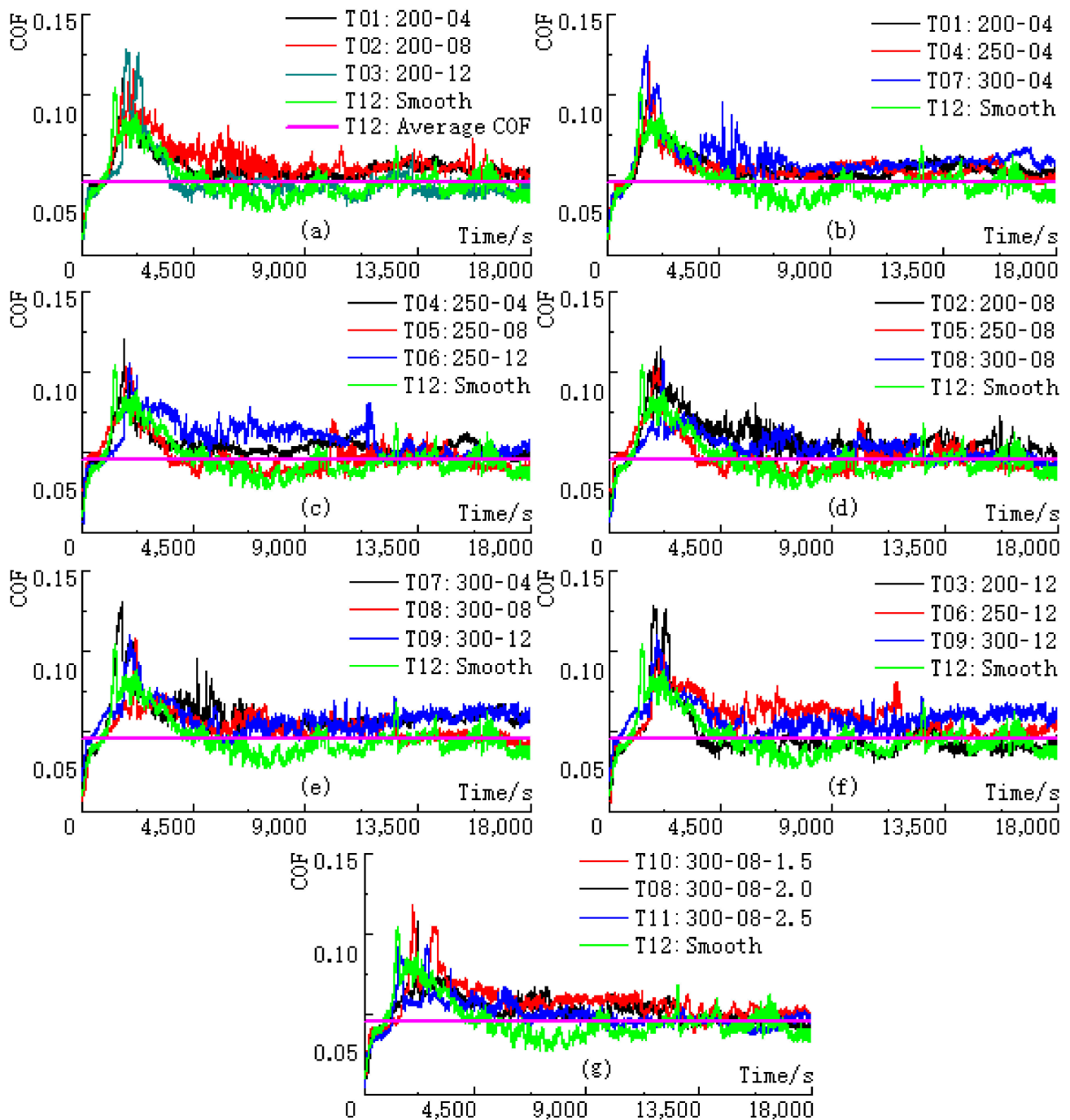
Figure 2. COFcurves of T01–T12 (**a**) bearings with a fixed DAOD of 200 μm, (**b**) bearings with a fixed DPOD of 4 μm, (**c**) bearings with a fixed DAOD of 250 μm, (**d**) bearings with a fixed DPOD of 8 μm, (**e**) bearings with a fixed DAOD of 300 μm, (**f**) bearings with a fixed DPOD of 12 μm, (**g**) bearings with different CFIAs.

Specifically, when the DAOD is fixed, with the increase inthe DPOD, the equivalent stresses increase and the difference between curves becomes more significant (see Figure 5a,c,e). The peak values onboth sides of raceways increase obviously, and the difference becomes more and more significant too. This is because when the DPOD becomes bigger, the dents will further deteriorate the integrity of the raceway of textured bearing. With the rolling of rollers, the adjacent region around the dents will be prone to generating large deformations, which then leads to high surface stresses, especially along the edges of dents.
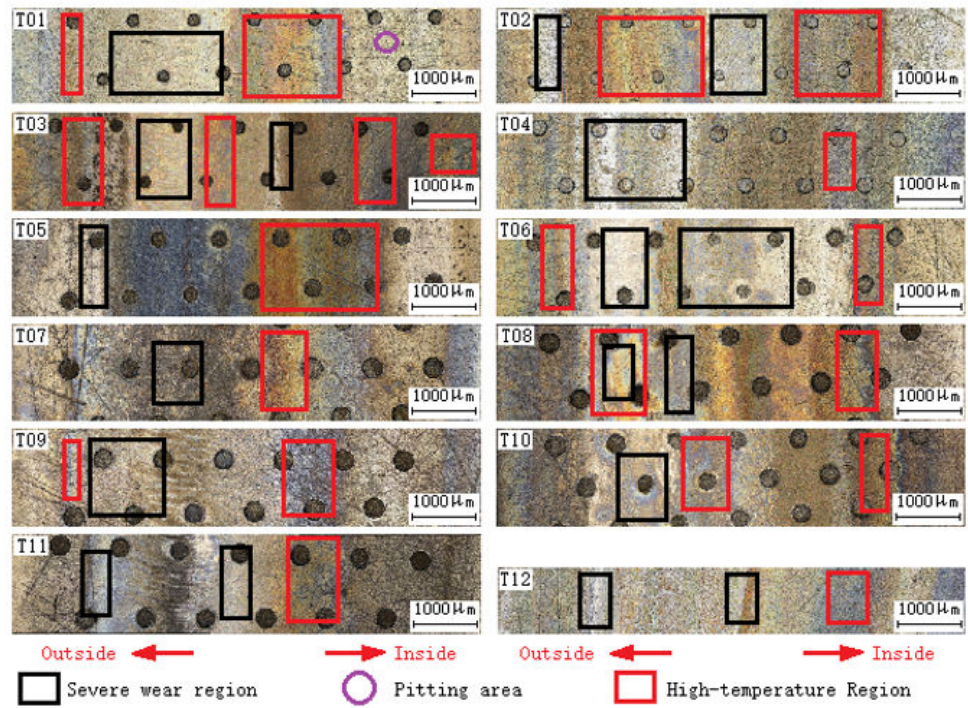
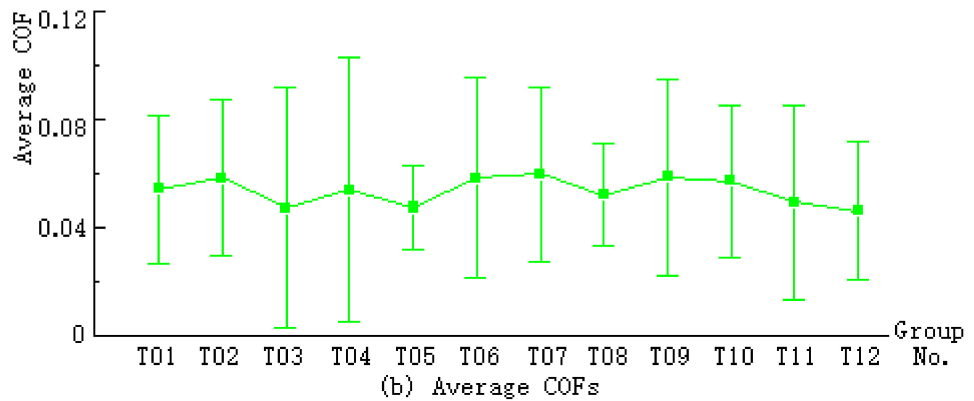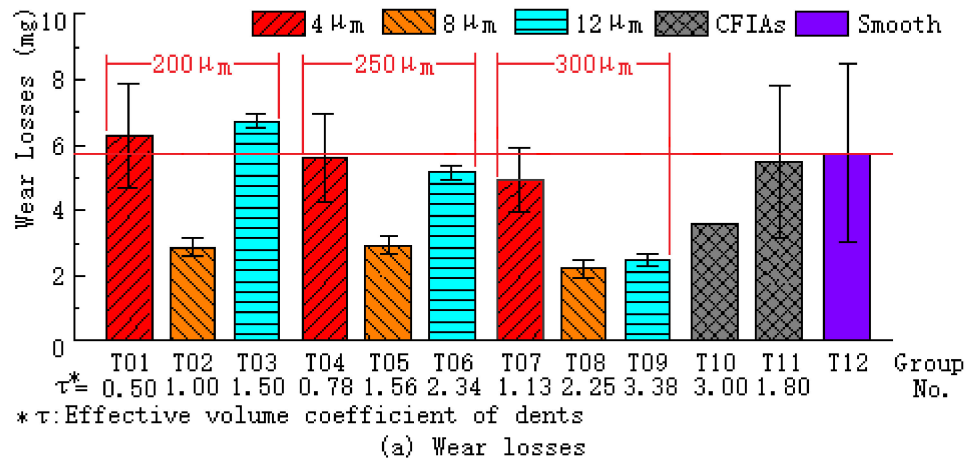**Figure 3.** Cleaned worn surfaces of the shaft washers of T01–T12.

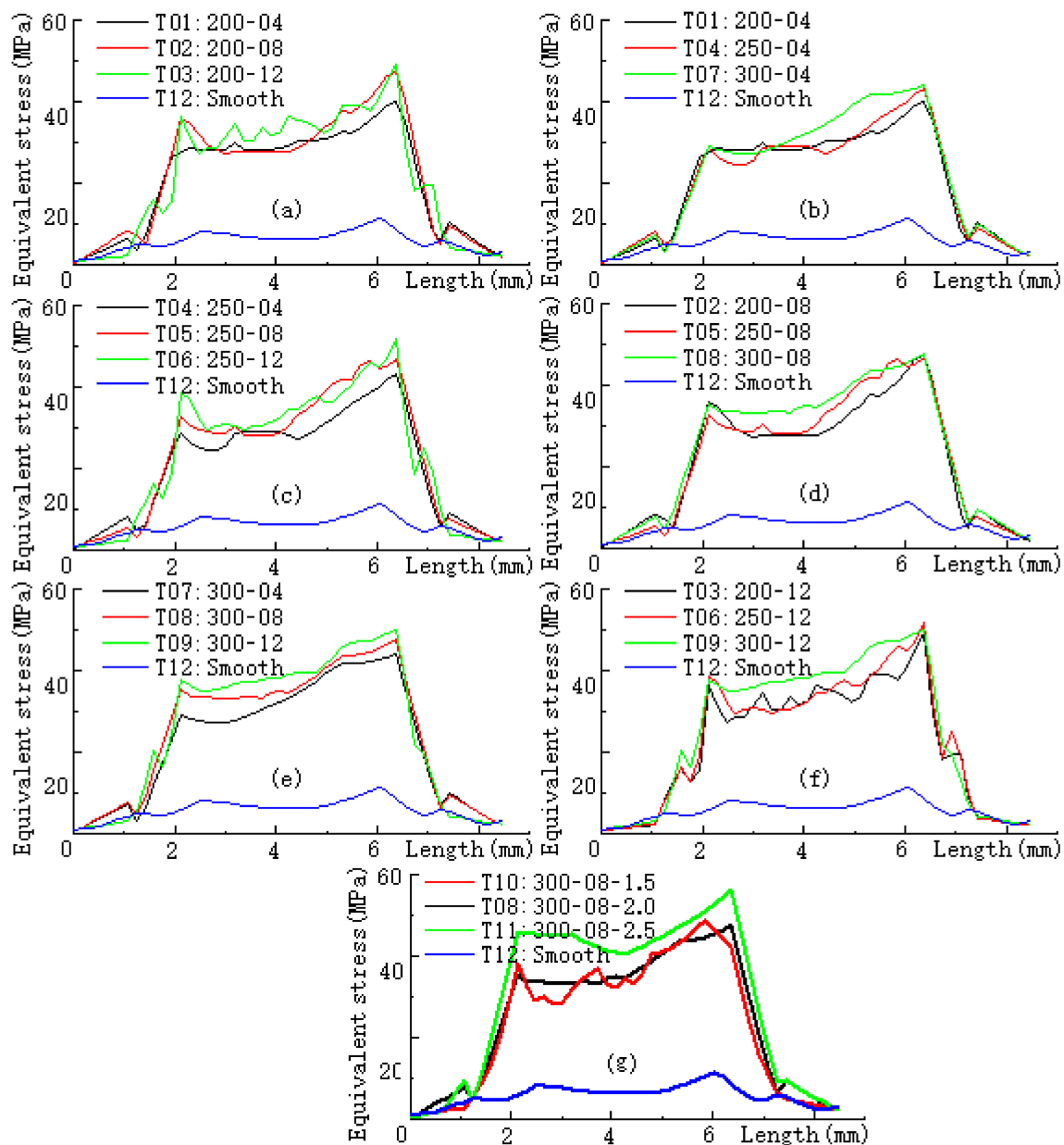**Figure 4.** Mass losses (shaft washers) and average-COFs of T1–T12.

Figure 5. Equivalent stress curves along the paths of T01–T12 (**a**) bearings with a fixed DAOD of 200 μm, (**b**) bearings with a fixed DPOD of 4 μm, (**c**) bearings with a fixed DAOD of 250 μm, (**d**) bearings with a fixed DPOD of 8 μm, (**e**) bearings with a fixed DAOD of 300 μm, (**f**) bearings with a fixed DPOD of 12 μm, (**g**) bearings with different CFIAs.

Similarly, when the DPOD is fixed (4, 8, or 12 μm), the equivalent stresses along the paths become bigger slowly, as the DAOD increases from 200 to 300 μm (see Figure 5b,d,f). This is because when the DPOD is constant, the effective contact area between the raceway and rollers becomes smaller with the increase in the DAOD, which will lead to high contact stresses on the textured raceway. The difference in curves is quite small, especially in the two peaks, indicating the weak effect of the DAOD on the surface stresses of the "washers-cage-rollers" system.

Figures 5g and 6 show the equivalent stress curves and contours of bearings (T10, T08, T11) with different CFIAs (1.5°, 2°, 2.5°), respectively. As shown in the figures, when the CFIAs are 1.5° and 2.0°, there is almost no apparent difference between the two curves or contours. When the CFIA is 2.5°, the equivalent stress of T11 is much higher than those of

T10 and T08 (see Figure 6c). Compared with the smooth group, the existence of CFIA means the reduced effective contact area of the "washers-cage-rollers" system, which will increase the surface stress of dents textured raceways. This is the reason for the high equivalent stress of T11. However, when the CFIA becomestoo small, the toughness of the textured surface will be weakened, and the contact stress will decrease instead. This is the reason for the low equivalent contact stresses of T10 and T08. So, there is a turning point in this work, 2°.
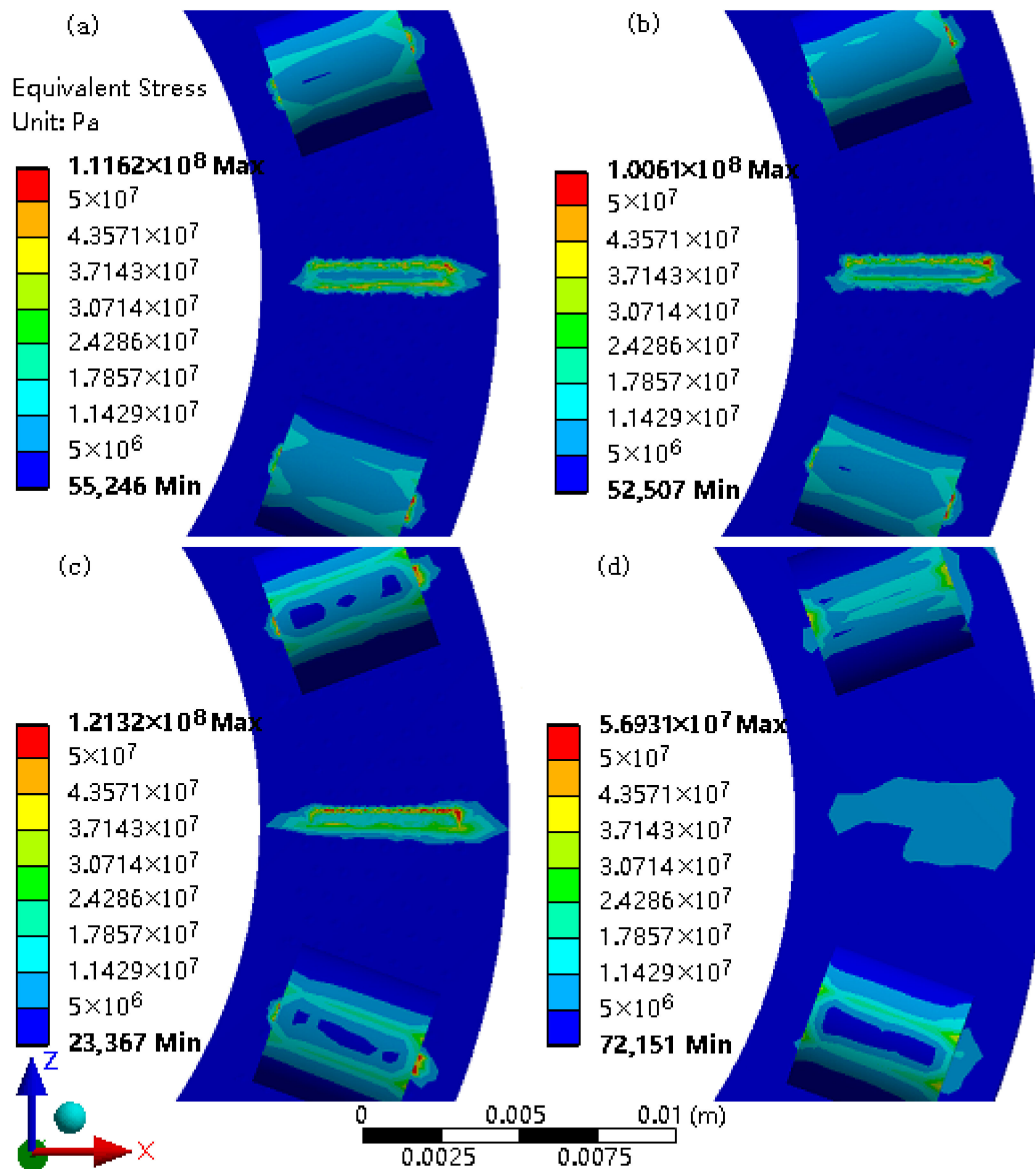

Figure 6. Equivalent stress contours of (**a**) T10, (**b**) T08, (**c**) T11, (**d**) T12.

4. Discussions

4.1. Effect of Pattern Parameters of Dents on the Tribological Behavior

4.1.1. DAODs and DPODs

As shown in Figure 2, when bearings are tested under dry wear, the difference of COF curves of bearings with fixed DAODs is gradually reduced with the increase inthe DPOD, while the difference of those curves with fixed DPODs becomes significant when the DAOD increases from 200 to 300 μm. Especially, when the DAOD is 200 μm, the fluctuation, and amplitude of the curves of T01, T02, and T03 aremuch different and they can be distinguished easily. When the DAOD is 300 μm, three curves are mixed and it is

very difficult to distinguish them, indicating the unapparent effect of the DPOD on the COFs in this condition. Likewise, as the DPOD is 4 μm, the DAOD has little influence on the fluctuation and amplitude of friction coefficients, and the three curves mix together. While the DPOD is 12 μm, the influence of the DAOD on the friction coefficient is significant, and three curves can be distinguished easily. Therefore, when the DAOD is small and the DPOD is big, the influence of pattern parameters on the curves is great. This is the reason for the relatively low average COFs of T03 and T05. On the contrary, when the DAOD is big and the DPOD is low, the influence of pattern parameters on the friction coefficients is unapparent. This is the reason for the relatively high average-COFs of T04 and T07. Among all textured bearings, the average-COF of T08 is moderate.

As for the peak delay phenomena, compared with the smooth group, the peak-times of dent COF curves of textured bearings all lag behind under dry wear (see Figure 2), due to the debris collection of dents. Among all dents textured bearings, the COF peaks of T06, T08, and T09 are delayed by about 500 s, and the peak-time of T11 lagsby about 800 s. Specifically, when the DAOD is fixed, the peak-time delays of bearings become much bigger when the DPOD changes from 4 to 12 μm. While the DPOD remainsfixed, the peak-time delays of groups are hard to be distinguished with the increase in DAOD. So, the influence of the DAOD on the peak-time delays of curves is strong, while that of the DPOD is not clear.

In the end, the wear losses of most dents textured bearings are smaller than that of the non-textured group (see Figure 4), except for T01 and T03. Specifically, when the DAOD remainsfixed, i.e., T01–T03, T04–T06, or T07–T09, with the variation of the DPOD, the mass losses of bearings are reduced first and then increase. The variation range is huge. Obviously, there is an inflection point of the DPOD. As the DPOD is fixed, like {T01, T04 and T07}, {T02, T05 and T08} or {T03, T06 and T09}, the losses of dents textured bearings decrease with the increase inthe DAOD, and the change is slow. Therefore, the DPOD has a great influence on the wear loss in this condition, while the effect of the DAOD on the wear volume is relatively small.

4.1.2. CFIAs

As shown in Figure 2g, the COF curves of T10, T08, and T11 are somewhat mixed, and their mass losses are all smaller than that of the non-textured group. As shown in Figure 4, the wear loss first decreases and then increases with the increase inthe CFIA, i.e., there is an inflection point. Among three CFIAs, the peak-time delay of T11 is the shortest and that of T08 is the longest; the average-COF of T11 is the lowest and that of T10 is the highest; the wear loss of T08 is the smallest, and that of T11 is the biggest.

This is because thesmall CFIA means big EVCD, i.e., large debris capacity of dents textured raceway. This is helpful to postpone the peak-times and further lower the COFs and wear losses of bearings. However, the minimum value of CFIA is determined by the DAOD and the texture area ratio to be obtained. When the CFIA becomestoo small, the toughness of the textured surface will be weakened, and the contact stress will decrease instead (see Figure 5). The effective contact area of the "washers-cage-rollers" system is also reduced. As a result, the wear loss of bearing will increase, especially under dry wear. On the contrary, when the CFIA becomesbigger, the effective contact area of the system, as well as the whole contact stress, increases significantly. This is a disadvantage to controlling the wear performance of dents textured bearing, and also the reason forthe high wear loss of T11. In this work, 2.0° is the turning point of the CFIA.

4.1.3. Summary

When bearings run under dry wear, the average-COFs of dents textured groups are all higher than that of non-textured one, their anti-wear properties may be becoming better or worse, which mainly depended on the combination of pattern parameters. Compared with the tribological data of the smooth group, the anti-wear properties of T02, T05, T08, and T09 are significantly improved (see Figures 3 and 4). The wear properties of T01 and T03

becomeworse. The wear loss of T08 is the lowest (2.21 mg). As shown in Figure 3, the wear marks mainly concentrate in the middle as well as the outsides of the worn raceways of bearings, whether the textured or smooth. Based on the worn surfaces, it can be found that fatigue pitting is the main wear mode of all groups, accompanied by slight abrasive wear.

Therefore, according to the above tribological data, the effect of pattern parameters on the tribological behavior of rolling element bearings under dry wear can be summarized and listed inthe following three situations: (1) As the DPOD is 4 μm, the debris collection capacity of dents is limited, and there istoo much nylon debris left in the "washers-cage-rollers" system, leading to the thickness increase inthe nylon film (see Figure 7e), which has been identified through the Fourier transform infrared spectroscopy (FTIR, IS10, Thermo Fisher Scientific, Waltham, MA, USA). The typical infrared characteristic spectrum of nylon can be observed [31,32]. The COF of nylon-to-GCr15 is greater than that of steel-to-steel, so the COFs of T01-T03 are all higher than that of the smooth group. Their wear losses are similar to the loss of T12 and even slightly higher. Their system temperatures rise rapidly and their final stabilized temperatures are very high, resulting in the test failure many times. (2) When the DAOD is 250 or 300 μm and the DPOD is 8 μm, the debris-collection ability of dents is moderate. The nylonpowder left in the system is few and the nylon film is quite thin and more uniform. Although their COFs (T05 and T08) are still higher than that of the non-textured group, their mass losses are much lower than that of T12. Correspondingly, their system temperatures rise slowly and their final stabilized temperatures are relatively lower than those of T01-T03. (3) As the DAOD is 250 or 300 μm, the DPOD is 12 μm, and the debris collection capacity of dents is greater than the nylon powder generated in the system. The nylon film becomes extremely thin and uneven. The COFs of bearings slightly increase compared with those of T05 and T08, and their mass losses are also slightly smaller than that of the smooth group. Their system temperatures rise fast and their final stabilized temperatures are much higher than those of T05 and T08.
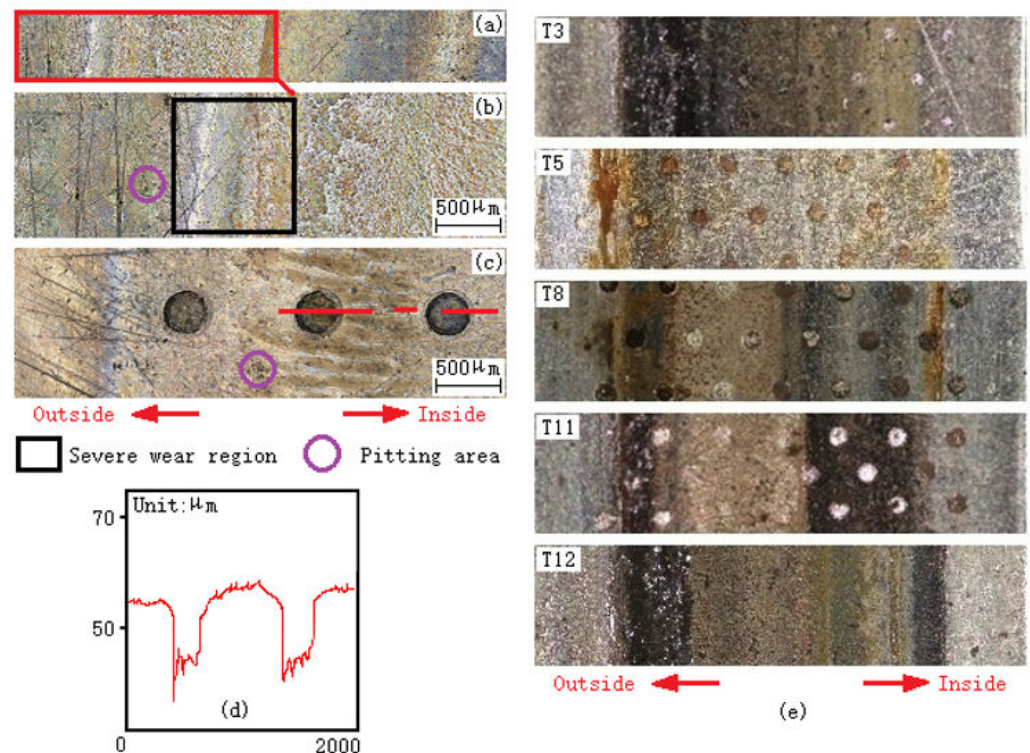

Figure 7. Worn surfaces of T03, T05, T08, T09, T11, and T12. (**a**) Worn surfaces of T12; (**b**) magnification of the red rectangle in (**a**); (**c**) worn surfaces of T09; (**d**) section curve of the crushed dent of (**c**); (**e**) nylon film of T03, T05, T08, T09, T11 and T12.

4.2. Influence Mechanism of Dents on the Tribological Properties under Dry Wear

There are sliding phenomena between the rollers and washers of TCRBs, so the maximum shear-stresses are inclined to the raceway of the washer. This will speed upthe initiation of surface fatigue cracks and accelerate the growth [36]. Therefore, the local material fatigue-pitting is the main metal debris source of the "washers-cage-rollers" system of rolling element bearings, both textured and smooth. In the meantime, owing to the high surface contact stresses, serious "edge collapse" phenomena occur along the edges of dents (see Figure 7d), resulting in an increase inwear debris, especially when the DPOD is 12 μm, which is another debris source of the textured bearings.

When 81107TN bearing runs under dry wear, the cylindrical rollers will contact directly with the pockets, whether textured or smooth. As a result, the serious wear of the nylon cage happens and abundant nylon powder is generated and left in the system. With the ongoing test, the system temperature rises gradually under the action of huge friction-induced heat. The nylon powder melts under local high temperatures, and an uneven nylon film gradually forms on the raceways of washers (both the shaft washer and seat washer), leading to a sharp increase inthe COF [29,32]. As the temperature of the "washers-cage-rollers" system rises, the pockets of the cage become much smoother than before, and the nylon film also becomes even and smooth. Finally, the system becomes balanced and the COF decreases very fast and becomes stable gradually (see Figure 2).

The influence mechanism of dents on the friction and wear properties of TCRBs under dry wear can be summarized as the following: compared with the smooth bearings, due to the "capture and collection of nylon powder" of dents, the nylon film on the textured raceway is more uniform (see Figure 7e). The metal debris from the "edge collapse" and fatigue spalling drop into the "washers-cage- rollers" system or melt into the nylon film [37]. Owing to the well mechanical properties, wear-resistance, and self-lubricity of nylon, the film can effectively isolate and protect the raceways. This will increase the COFs of bearings and decrease their mass losses. In addition, the raceway material can be seen as numerous micro-cantilever-beams [28,29]. The increase inthe DPOD means the increase inthe length of those micro-cantilever-beams. Based on the theoretical mechanics and the frictional characteristics of the TCRBs, rolling combined with sliding, will significantly increase the shear stress of the surface material, especially along the edges of dents. This is the reason forthe serious "edge collapse" phenomena when the DPOD is 12 μm (see Figure 7c,d). The EVCD is a key parameter to determine the values of the COFs of dents textured bearings, but the effect of EVCD on the tribological performance of dents textured bearings lacks regularity in this condition.

5. Conclusions

Based on the above data under dry wear, the following conclusions could be drawn:

1. The average-COFs of dents textured bearings are all higher than that of the non-textured group. Their wear losses are bigger or smaller than that of smooth, depending on the combination of the DAOD and DPOD. The DPOD has a great influence on the COFs and the wear losses of TCRBs. The influence of the DAOD on the COFs as well as the wear losses is relatively small. When the DAOD is small and the DPOD is high, their effect on the COF is strong.

2. The existence of nylon film can significantly increase the COF of the "washers-cage-rollers" system, protect the textured surfaces, and further reduce the wear loss of bearings. Fatigue pitting is the main wear mode of bearings, accompanied by slight abrasive wear.

3. Small CFIA is helpful to postpone the peak-time under dry wear and further lower the COFs and wear losses of dents textured TCRBs. However, when the CFIA is too small, the toughness of the textured surface will be weakened. In this work, 2.0° is the turning point of the CFIA.

4. Compared with the smooth group, the equivalent stresses of textured bearings are 4~5 times larger and their peak stresses can be even up to 53.37 MPa. So, the friction

and wear properties of dents textured TCRBs are determined by the following factors: surface stress distribution, nylon film characteristics (thickness and flatness), "local quenching" effect, "edge collapse", loads, etc. In this work, when the DAOD and the DPOD are 250 and 8 μm, respectively, compared with the non-textured group, the wear loss of dents textured TCRBs could be reduced by up to 49.22% under dry wear.

This work will be an important reference for the optimal design of the raceways of REBs.

Author Contributions: Analysis of data, S.S.; formal analysis, S.S.; writing-original draft, S.S.; conceptualization, R.L.; visualization, R.L.; writing—review & editing, R.L. and X.D.; project administration, Z.J. (Zhihao Jin); resource, Z.J. (Zhihao Jin); supervision, Z.J. (Zhihao Jin) and Y.Z.; methodology, Y.Z.; funding acquisition, Y.Z.; data curation, Z.J. (Zichen Ju); software, Z.J. (Zichen Ju); tests, Z.J. (Zichen Ju). All authors have read and agreed to the published version of the manuscript.

Institutional Review Board Statement: Not applicable.

Informed Consent Statement: Not applicable.

Data Availability Statement: The data presented in this study are available on request from the corresponding author.

Conflicts of Interest: The authors declare that there are no conflict of interest regarding the publication of this paper.

References

1. Nehme, G.N. Tribological behavior and wear prediction of molybdenum disulfide grease lubricated rolling bearings under variable loads and speeds via experimental and statistical approach. *Wear* **2017**, *376–377*, 876–884. [CrossRef]
2. Hsu, C.J.; Stratmann, A.; Medina, S.; Jacobs, G.; Mücklich, F.; Gachot, C. Does laser surface texturing really have a negative impact on the fatigue lifetime of mechanical components? *Friction* **2021**, *9*, 1766–1775. [CrossRef]
3. Jacobs, W.; Hooreweder, B.V.; Boonen, R.; Sas, P.; Moens, D. The influence of external dynamic loads on the lifetime of rolling element bearings: Experimental analysis of the lubricant film and surface wear. *Mech. Syst. Signal. Process.* **2016**, *74*, 144–164. [CrossRef]
4. Rosenkranz, A.; Grützmacher, P.G.; Gachot, C.; Costa, H.L. Surface texturing in machine elements—A critical discussion for rolling and sliding contacts. *Adv. Eng. Mater.* **2019**, *21*, 1900194. [CrossRef]
5. Long, R.S.; Sun, S.N.; Zhang, Y.W. Wear behavior of pits textured grey cast iron rings with Zr/ZrN coatings under dry sliding. *Proc. Inst. Mech. Eng. J.-J. Eng. Tribol.* **2021**, *235*, 1251–1261. [CrossRef]
6. Gachot, C.; Rosenkranz, A.; Hsu, S.M.; Costa, H.L. A critical assessment of surface texturing for friction and wear improvement. *Wear* **2017**, *372–373*, 21–41. [CrossRef]
7. Yuan, Z.W.; Qin, Y.; Deng, C.L.; Zheng, P. Synergistic effects of surface strengthening and surface micro-texture on aviation spherical plain bearing tribological properties. *Proc. Inst. Mech. Eng. J.-J. Eng. Tribol.* **2018**, *232*, 797–808. [CrossRef]
8. Galda, L.; Sep, J.; Olszewski, A.; Zochowski, T. Experimental investigation into surface texture effect on journal bearings performance. *Tribol. Int.* **2019**, *136*, 372–384. [CrossRef]
9. Wang, L.L.; Guo, S.H.; Wei, Y.L.; Yuan, G.T.; Geng, H. Optimization research on the lubrication characteristics for friction pairs surface of journal bearings with micro texture. *Meccanica* **2019**, *54*, 1135–1148. [CrossRef]
10. Ahmadkhah, A.; Kakaee, A.H. Three-dimensional thermohydrodynamic investigation on the micro- groove textures in the main bearing of internal combustion engine for tribological performances. *Proc. Inst. Mech. Eng. J.-J. Eng. Tribol.* **2021**, *235*, 854–869. [CrossRef]
11. Kumar, V.; Sharma, S.C. Influence of dimple geometry and micro-roughness orientation on performance of textured hybrid thrust pad bearing. *Meccanica* **2018**, *53*, 3579–3606. [CrossRef]
12. Hu, D.; Guo, Z.W.; Xie, X.; Yuan, C.Q. Effect of spherical-convex surface texture on tribological performance of water-lubricated bearing. *Tribol. Int.* **2019**, *134*, 341–351. [CrossRef]
13. Touche, T.; Cayer-Barrioz, J.; Mazuyer, D. Friction of textured surfaces in EHL and mixed lubrication: Effect of the groove topography. *Tribol. Lett.* **2016**, *63*, 25. [CrossRef]
14. Zhang, D.Y.; Gao, F.; Wei, X.; Liu, G.L.; Hua, M.; Li, P.Y. Fabrication of textured composite surface and its tribological properties under starved lubrication and dry sliding conditions. *Surf. Coat. Technol.* **2018**, *350*, 313–322. [CrossRef]

15. Xu, Y.F.; Zheng, Q.; Abuflaha, R.; Olson, D.; Furlong, O.; You, T.; Zhang, Q.Q.; Hu, X.G.; Tysoe, W.T. Influence of dimple shape on tribofilm formation and tribological properties of textured surfaces under full and starved lubrication. *Tribol. Int.* **2019**, *136*, 267–275. [CrossRef]

16. Zhang, D.Y.; Zhao, F.F.; Wei, X.; Gao, F.; Li, P.Y.; Dong, G.N. Effect of texture parameters on the tribological properties of spheroidal graphite cast iron groove-textured surface under sand-containing oil lubrication conditions. *Wear* **2019**, *428–429*, 470–480. [CrossRef]

17. Gherca, A.; Fatu, A.; Hajjam, M.; Maspeyrot, P. Influence of surface texturing on the hydrodynamic performance of a thrust bearing operating in steady-state and transient lubrication regime. *Tribol. Int.* **2016**, *102*, 305–318. [CrossRef]

18. Kümmel, D.; Hamann-Schroer, M.; Hetzner, H.; Schneider, J. Tribological behavior of nanosecond-laser surface textured Ti6Al4V. *Wear* **2019**, *422–423*, 261–268. [CrossRef]

19. Saeidi, F.; Parlinska-Wojtan, M.; Hoffmann, P.; Wasmer, K. Effects of laser surface texturing on the wear and failure mechanism of grey cast iron reciprocating against steel under starved lubrication conditions. *Wear* **2017**, *386–387*, 29–38. [CrossRef]

20. Lenart, A.; Pawlus, P.; Dzierwa, A. The effect of steel disc surface texture in contact with ceramic ball on friction and wear in dry fretting. *Surf. Topogr. Metrol.* **2018**, *6*, 034004. [CrossRef]

21. Koike, H.; Kida, K.; Mizobe, K.; Shi, X.C.; Oyama, S.; Kashima, Y. Wear of hybrid radial bearings (PEEK ring-PTFE retainer and alumina balls) under dry rolling contact. *Tribol. Int.* **2015**, *90*, 77–83. [CrossRef]

22. Morales-Espeje, G.E.; Gabelli, A. Rolling bearing performance rating parameters: Review and engineering assessment. *Proc. Inst. Mech. Eng. J.-J. Eng. Tribol.* **2020**, *234*, 3064–3077. [CrossRef]

23. El-Thalji, I.; Jantunen, E. A descriptive model of wear evolution in rolling bearings. *Eng. Fail. Anal.* **2014**, *45*, 204–224. [CrossRef]

24. Winkler, A.; Marian, M.; Tremmel, S.; Wartzack, S. Numerical modeling of wear in a thrust roller bearing under mixed elastohydrodynamic lubrication. *Lubricants* **2020**, *8*, 58. [CrossRef]

25. Rosenkranz, A.; Stratmann, A.; Gachot, C.; Burghardt, G.; Jacobs, G.; Mücklich, F. Improved wear behavior of cylindrical roller thrust bearings by three-beam laser interference. *Adv. Eng. Mater.* **2016**, *18*, 854–862. [CrossRef]

26. Vidyasagar, K.E.C.; Pandey, R.K.; Kalyanasundaram, D. Improvement of deep groove ball bearing's performance using a bionic textured inner race. *J. Bionic. Eng.* **2021**, *18*, 974–990. [CrossRef]

27. Vidyasagar, K.E.C.; Pandey, R.K.; Kalyanasundaram, D. An exploration of frictional and vibrational behaviors of textured deep groove ball bearing in the vicinity of requisite minimum load. *Friction* **2021**, *9*, 1749–1765. [CrossRef]

28. Long, R.S.; Zhao, C.; Jin, Z.H.; Zhang, Y.M.; Pan, Z.; Sun, S.N.; Gao, W.H. Influence of Groove Dimensions on the Tribological Behavior of Textured Cylindrical Roller Thrust Bearings under Starved Lubrication. *Ind. Lubr. Tribol.* **2021**, *73*, 971–979. [CrossRef]

29. Long, R.S.; Pan, Z.; Jin, Z.H.; Zhang, Y.M.; Sun, S.N.; Wang, Y.Y.; Wang, Y.B.; Li, M.H. Tribological behavior of grooves textured thrust cylindrical roller bearings under dry wear. *Adv. Mech. Eng.* **2021**, *13*, 16878140211067284. [CrossRef]

30. Long, R.S.; Zhao, C.; Zhang, Y.M.; Wang, Y.B.; Wang, Y.Y. Effect of vein-bionic surface textures on the tribological behavior of cylindrical roller thrust bearing under starved lubrication. *Sci. Rep.* **2021**, *11*, 21238. [CrossRef] [PubMed]

31. Long, R.S.; Shang, Q.Y.; Jin, Z.H.; Zhang, Y.M.; Ju, Z.C.; Li, M.H. Tribological behavior of laser textured rolling element bearings under starved lubrication. *Ind. Lubr. Tribol.* **2022**. [CrossRef]

32. Long, R.S.; Li, M.H.; Jin, Z.H.; Zhang, Y.M.; Han, H. Tribological behavior of pits textured multi-rollers sliding-rolling tribo-pair under periodic varied load and dry wear. *Adv. Mech. Eng.* **2022**, *14*, 092520. [CrossRef]

33. Marian, M.; Weikert, T.; Tremmel, S. On friction reduction by surface modifications in the TEHL cam/tappet- contact-experimental and numerical studies. *Coatings* **2019**, *9*, 843. [CrossRef]

34. Long, R.S.; Kelly, P.; Sun, S.N.; Feng, J.L.; Wang, X.W.; Li, W.Y. The influence of pits on the tribological behavior of grey cast iron under dry sliding. *Math. Probl. Eng.* **2018**, *2018*, 8767895. [CrossRef]

35. Sun, S.N.; Long, R.S.; Zhang, Y.M.; Li, M.H. The influence of initial deflection angle on the tribological properties of gray cast iron rings with curve distributed pits under dry sliding. *Proc. Inst. Mech. Eng. J.-J. Eng. Tribol.* **2021**, *235*, 1659–1668. [CrossRef]

36. Wen, S.Z.; Huang, P. *Principles of Tribology*, 4th ed.; Tsinghua University Press: Beijing, China, 2012. (In Chinese)

37. Grützmacher, P.G.; Rosenkranz, A.; Rammacher, S.; Gachot, C.; Mücklich, F. The influence of centrifugal forces on friction and wear in rotational sliding. *Tribol. Int.* **2017**, *116*, 256–263. [CrossRef]